The IRM Quarterly
Spring 2002, Vol. 12, No. 1

Seahenge, Susceptibility,

and more ways to be wrong

Neil Linford
English Heritage
Mike Jackson
Jim Marvin
IRM

Discovered in August 1999, a rough circle (diameter ~6m) of timber posts surrounding a large upturned oak tree stump became known as "Seahenge" in deference to its Bronze Age contemporary, Stonehenge. Photograph reproduced with the kind permission of the Norfolk Archaeological Service.

Seahenge reappeared, rather unexpectedly, from the sea in an area of shifting sand and peat deposits on the beach close to the village of Holme-next-the-sea, Norfolk, UK. Obviously, such well preserved sites are comparatively rare within the archaeological record and it was decided, not without a degree of controversy, to stage a total excavation of the monument. Dating evidence, including the recovery of a bronze hand axe and a novel combination of dendrochronology combined with radiocarbon determinations, suggested the central oak tree stump was felled in the summer of 2050BC and the surrounding circle of timber posts in the following year [*Bayliss, Groves et al*. 2000].

The precise form and function of the monument remains a matter of some speculation, but it seems likely that the original circle of timber posts might have risen to a height of at least 2 or 3m surrounding the platform created by the central upturned oak stump. One rather gruesome interpretation proposes the site may have been used for the ritual excarnation of the deceased, where bodies would be left exposed to the elements, birds and wild animals to strip the flesh from the bones in the open air, liberating the dead person's spirit

Whilst magnetic measurements of the sediments surrounding Seahenge are unlikely to reveal much direct evidence for the funereal practises of Bronze age man it was hoped they might provide some useful information regarding site formation and construction processes.

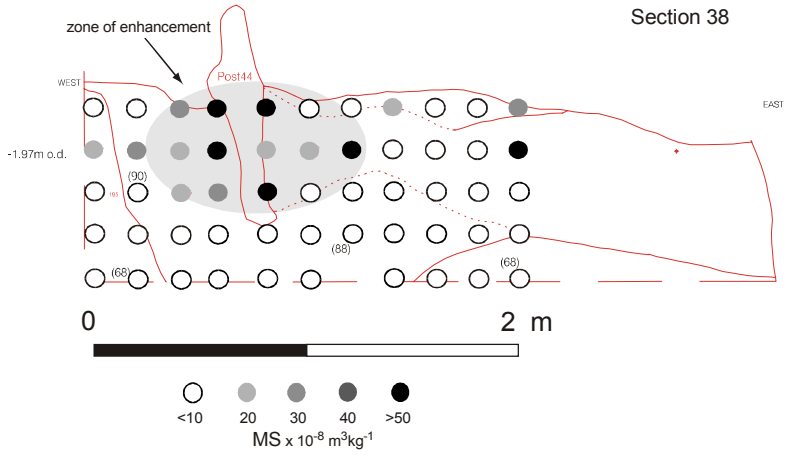

Fig. 1. A significant degree of magnetic enhancement is associated with surviving timber posts (vertical E-W profile and sampling grid for magnetic specimens).

The presence of burnt material within the buried soils surrounding the monument might also be detected magnetically [*e.g., Linford* 1999] and could, perhaps, provide a further insight to the use of the timber circle.

Initial measurements of magnetic susceptibility revealed a zone of enhancement surrounding the location of the timber posts (Fig 1), possibly indicating the remains of contemporary topsoil repacked into a trench cut to receive the upstanding timbers. Alternatively, the timbers may have been driven directly into the ground surface without first excavating a pit or trench. If this were the case the magnetisation would be unrelated to the former topsoil and might, perhaps, be formed through the post-depositional diagenesis of iron

Seahenge... *continued on p. 9*

On Data Analysis & Interpretation, Part 4
Previous installments:
10(4) χ_{fd} and superparamagnetism (de Wall & Worm)
11(1) low-T FORC analysis (Pike & Marvin)
11(4) sample size and shape effects (IRM)

Mechanisms of Magnetization Studied by Low-Temperature FORC Analysis

Helmut G. Katzgraber, Kai Liu and Christopher Pike
UC Davis Physics Dept.
dummkopf@physics.ucdavis.edu

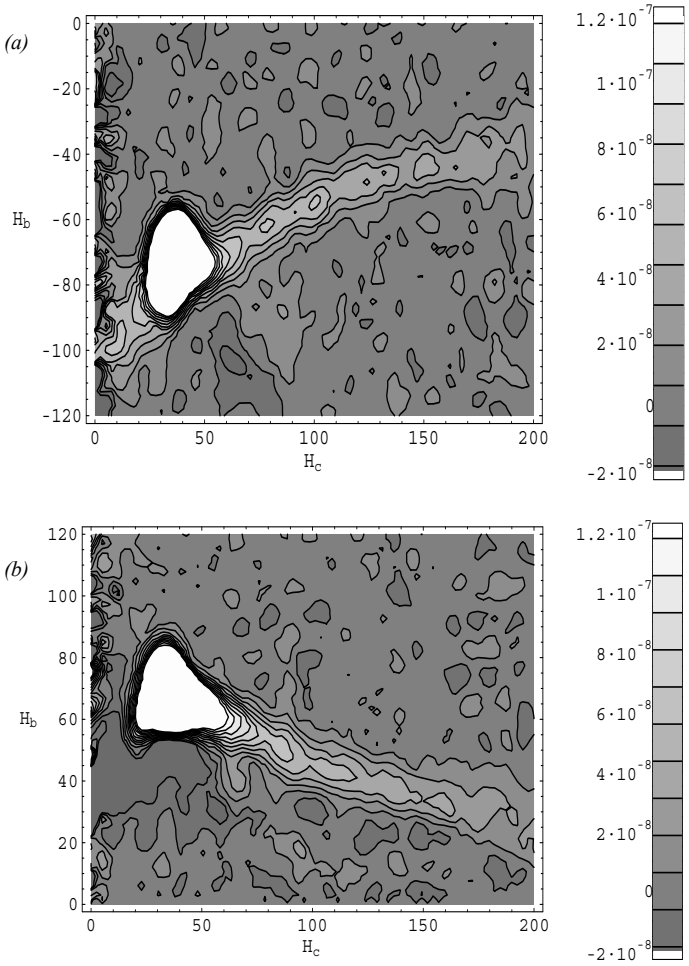

Fig 1. FORC diagrams for an exchange-biased Fe/FeF_2 bilayer thin film at 50 K, along the increasing (a) and decreasing (b) branches of the hysteresis loop.

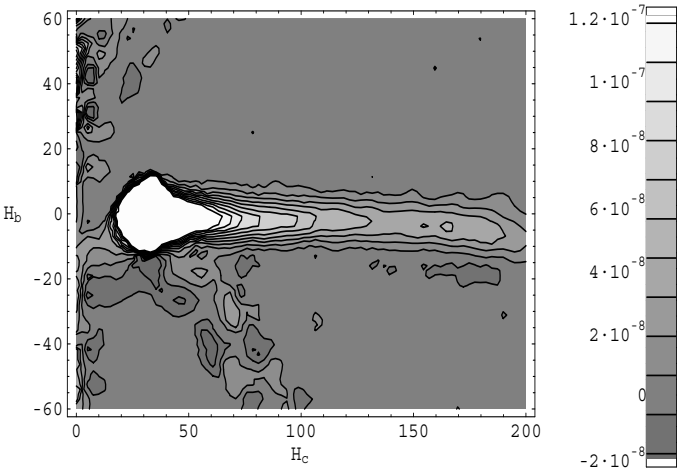

Fig 2. FORC diagram for the Fe/FeF_2 bilayer thin film at 100 K, above the Néel point of the FeF_2, where exchange bias is absent.

1. Exchange-biased ferromagnet / antiferromagnet (FM/AF) bilayers

We have investigated the exchange-bias phenomenon, particularly the details of the magnetization reversal processes, in a Fe/FeF_2 bilayer thin film that exhibits a shifted hysteresis loop below the FeF_2 Néel temperature of 80K. The following experiments were carried out:

a) FORC measurements at T = 50K (Fig 1) and T = 100K (Fig 2) were performed, below and above the FeF_2 Néel temperature to compare the magnetization reversal mechanisms with and without the exchange bias.

b) At T = 50K, FORC measurements along increasing- and decreasing-field branches of the magnetic hysteresis loop (Fig 2a and 2b, respectively) were taken to search for different reversal mechanisms, in particularly to compare with earlier neutron scattering experiments that revealed magnetization rotation and domain wall motion along the two branches.

c) At T = 50K, magnetic hysteresis loops were measured as a function of in-plane angle between the magnetic field and the anisotropy axis. This will allow us to map out the angular dependence of the exchange field and the coercivity.

d) The temperature dependence of the magnetic hysteresis loop was measured which showed an increased switching sharpness approaching the FeF_2 Néel temperature.

2. Ion irradiated samples

We performed FORC measurements in $Al/Fe/MnF_2/ZnF_2$ layered systems with and without ion irradiation to study if the noise in the measurements can be reduced by "pinning" magnetic domains with ion tracks.

Results show that there is little effect from the ion pin-sites in the noise seen in the hysteresis loops and FORC diagrams.

3. Single ferromagnetic layers

We performed FORC measurements with the low- and room-temperature VSM in order to compare to previous results obtained from AGM measurements on single-layer Co, Ni, Fe samples. We see that the noise level is reduced if we cool the systems to 80K. The data compare well to previous results and show more intricate details in the FORC diagrams which were not visible with the AGM at UC Davis.

4. Co vs. exchange-biased Co/FeMn

Co/FeMn shows exchange biasing at room temperature. The magnetic hysteresis loops were measured as a function of in-plane angle between the magnetic field and the anisotropy axis in oder to map out the angular dependence of the exchange field and the coercivity.

A FORC diagram for the Co samples was measured at room temperature.

5. Spin-glass systems

We have measured FORC diagrams for $KMnF_3$, a system known to have Heisenberg symmetry and known to undergo a spin-freezing transition at approximately 80K. We intend to compare our results to theoretical models to better understand the qualitative properties of the FORC method.

Preliminary results show that the system has spin-glass behavior due to domain-wall reorganization in the sample.

6. Well-dispersed single-domain recording media

We measured FORC diagrams as a function of temperature for a Kodak recording media sample (Co-γ-Fe_2O_3) to see if low temperatures have an influence on thermal fluctuations of the easy axes of the particles.

We find that low temperatures freezes the fluctuations increasing the resolution in FORC diagrams.

7. Geological samples

C. Pike (UC Davis Geology) measured FORC diagrams of geological (Chinese Loess, flyash) samples. Results were not available at the time of this communication.

We would like to thank the staff at the IRM for their help and hospitality.

BangYeon Kim
Lehigh University
bak4@lehigh.edu

Environmental magnetic study of Lake Ely, PA

Lake Ely is a small post-glacial lake in Pennsylvania that has annual sediment layers of alternating dark organics or light colored silt. Previous studies on the sediments from the lake showed a correlation between magnetic mineral concentration and local rainfall record over the past 65 years. In a simple erosional model, more rainfall would cause more erosion from the watershed, thus more input of magnetic grains into the sediments, and more magnetic silt-rich layers. However, the samples with dominantly dark organic-rich layers yielded higher SIRM than those with predominantly silt-rich layers.

Mineral magnetic measurements also suggest that the lake sediment magnetic minerals were formed in the lake. From the S-ratios and thermal demagnetization of the samples, magnetite was shown to be the main magnetic carrier in the lake sediments while watershed soil samples showed the presence of high coercivity antiferromagnetic minerals like hematite. Magnetosomes produced by magnetotactic bacteria would explain the enrichment of magnetite in the organic-rich layers. If this were true, it would offer an interesting insight to the link between rainfall and the productivity in the lake.

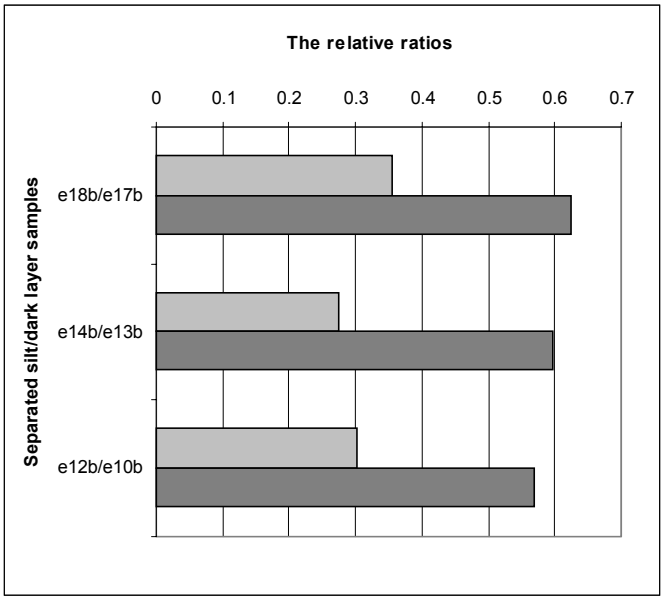

Figure 1. The contribution from the magnetosomes in the lake sediment samples obtained from the deconstruction of the low temperature data. The darker and lighter bars respectively represent the dark, organic rich samples, and the silt-rich samples. Note the dark samples have significantly higher contributions from biogenic magnetites.

Magnetotactic bacteria were observed in water pumped at the depth of the oxic-anoxic transition zone (OATZ) in the water column. This supports our contention that magnetite concentration variation could be caused by variations in bacterial productivity. Characterization of the varved sediment layers then became the focus of our study at *IRM*. A slab of the sediment freeze-core was freeze-dried, and dark-organic rich sediments and silt-rich sediments were separated. These samples could only be produced in small quantities ranging from tens to hundreds of mg. This amount was enough to fill the gel capsules used as sample holders for the MPMS measurements. The low temperature behavior was measured by MPMS. Frequency dependence of susceptibility, Curie temperature, and hysteresis parameters were also measured.

For the low temperature behavior data, the original idea was to apply the test proposed by Moskowitz et al. (1993) for the presence of magnetosomes. Since our samples are natural lake sediments, the Verwey transition was attenuated to varying degrees and the ratios between FC (field cooled) and ZFC (zero-field cooled) SIRMs were around 1.5, which is smaller than the ratios from the pure cultured magnetosomes. However, Carter-Stiglitz et al. (2001) have developed a technique to estimate the contribution from the different magnetic carriers in a sample to their low temperature behavior. Brian Carter-Stiglitz kindly ran some pilot data from Lake Ely as well as giving us a copy of the program. The low temperature SIRM curves were deconstructed using the type curves of magnetite from magnetosomes (MS1), greigite, superparamagnetic grains from GS15 and Ferrofluid, and goethite in order to determine the relative contribution of each of these minerals to the low temperature curves. The results of this analysis are presented in Figure 1. When a pair of adjacent dark and silt samples are compared, the contribution of the magnetosomes is always higher in dark, organic-rich samples, although silt-rich samples do have some small contributions from magnetosomes. This is important magnetic evidence for the presence of magnetosomes in the sediment. These results are confirmed by transmission electron microscopy (TEM) observations of magnetic extracts, which were performed after the low temperature magnetic measurements at *IRM*.

Room temperature measurements were not as diagnostic as the low temperature measurements. Frequency dependence of susceptibility had values smaller than 7% and some dark samples had negative numbers (-0.4% and -2.8%). Curie temperature measurements were not successful because heating always created secondary magnetic minerals that started to form at ~420° C, peaked at 480° C, and lost their intensity by 580° C. The formation of a magnetic mineral is common during heating of samples with a high organic content. Possibly sulphide and hydroxide minerals were converted to magnetite during the heating. A Day plot of hysteresis parameters shows that Mr/Mrs ratios are between 0.19 and 0.35, and Hcr/Hc ratios are between 1.84 and 2.91. Most of the grains fall in the upper left corner of the pseudosingle domain field in the Day plot.

In summary, the low temperature data were most diagnostic data collected from this visit to *IRM*. Dark, organic-rich samples showed higher contributions of the biologically produced magnetites.

I thank all the people in *IRM* for their support and help during the visit.

References

Carter-Stiglitz, B.S., Moskowitz, B.M. and Jackson, M.J., (2001). Unmixing magnetic assemblages, and the behavior of bimodal mixtures. *J. Geophys. Res., 106*, B11, 26,397-26,411.

Moskowitz, B.M., Frankel, R.B. and Bazylinski, D.A., (1993). Rock magnetic criteria for the detection of biogenic magnetite, *Earth Planet. Sci. Lett., 120*, 283-300.

Reports... *continued on p. 4*

Valentina Shcherbakova
Borok Geophysical Observatory.
shcherb@borok.adm.yar.ru

Analysis Of Mechanisms Causing the Thermal Pre-History Dependence of Value And Stability of pTRM in MD and PSD Samples

The general objective of my visit to the IRM was an experimental study of factors determining the difference in value and stability of $pTRM(T_1,T_2)$, acquired from different magnetic states determined by their thermal pre-history. For example, the $pTRM(T_1,T_2)$ can be imparted after heating a sample to T_c followed by cooling to T_1 in zero field. Alternatively, the sample can be cooled in zero field from T_c to room temperature T_r, then heated to T_1, whereupon $pTRM(T_1,T_2)$ is acquired between T_1 and T_2, followed by cooling the sample to T_r in zero field (if $T_2 > T_r$). The difference between these two cases is that the top temperature T_1 is reached by cooling from T_c (the first case) or by heating from T_r to T_1 (the second case). To distinguish between them, the notations $pTRM_a$ (the pTRM acquired by cooling to T_1 from *above*) for the first case and $pTRM_b$ (the pTRM acquired by heating to T_1 from *below*) for the second case are used here. As known, for these two kinds of pTRMs the relationship $pTRM_a > pTRM_b$ is valid (*Shcherbakov et al*. 1993, *Shcherbakova et al*., 2000).

For brevity, let us denote the corresponding magnetic states as the state "A" if T_1 is achieved by cooling from T_c or the state "B" if T_1 is achieved by heating from T_r. Besides, let us introduce the state "AF" which means that the specimen was AF demagnetized at $T = T_1$. As shown by *Shcherbakov et al* (2001),

$$pTRM_a(T_1,T_2) > pTRM_b(T_1,T_2) \geq pTRM_{af}(T_1,T_2). \quad (1)$$

It is very likely that this inequality must be linked to the different degree of stability (or metastability) of the domain state (DS) resulting from the prehistories A, B and AF. Thus, I thought that a natural way to prove this statement would be a comparison of IRM acquisition curves obtained from these states. Indeed, on account of the inequality(1) it follows that in relation to the acquisition of pTRM the hierarchy of stability of the three states is as follows:

AF is more stable than B
which, in turn, is more stable than A. (2)

The immediate goal of the experiments was to find out whether or not the same hierarchy is kept for the IRM(H) acquisition. Here H is the external magnetic field.

For this purpose, a set of 10 samples with well established magnetic characteristics was used for the study of the IRM(H) curves. The experiments were carried out on the high-temperature VSM, which seems to be perfect for such experments, as it has ability to produce all three magnetic states A, B and AF both at room and elevated temperatures. It is important that the samples are chemically stable to the thermal treatment and their DS ranges from SD to MD. The DS was identified according to their hysteresis parameters and relative value of the tail of pTRM(300°C, T_r) using the so-called thermomagnetic criterion (Shcherbakova et al., 2000). Specifically, the experimental part included first heating the samples in nonmagnetic space to T_c, with subsequent cooling to T_i (A-state) followed by measurements of the IRM(H) curve. Similarly, I proceeded with the creation of IRM(H) curves from the B- and AF-states. The temperatures T_i were chosen as 200°C, 300°C, 350°C, 400°C, 450°C, 500°C, 550° and even 600° - for the samples the contaning hematite. The maximum external DC field was (20 - 60) mT, though for one magnetically hard specimen the amplitude was increased up to100mT.

The only specimen for which the IRM(H) curves obtained for the A- and B-states were indistinguishable, is the SD specimen 16 - all other specimens are classified as PSD or MD. For them the following tendencies were noticed.

1. In general, the results of the experiments were as expected - the IRM(H) curves obtained from the AF-state, indeed, lie significantly below the corrsponding curves obtained from the A - and B- states, though the difference diminishes when T_i increases.

2. The difference between the curves obtained from the A - and B- states is detectable but much less pronounced than that of the previous statement (Fig1a, Fig.1b).

3. At low fields the IRM(H) curves obtained from the same state but at different T_i, are usually close each other until Ti does not exceed 500°C (Fig.2a, Fig.2b).

The conclusion which can be drawn from the experiments is that the basic hysteresis properties of the A- and B-states differ only slightly from one another even for MD samples, despite the fact that MD pTRMs obtained from these states differ significantly. It can be interpreted by such a way, that the magnetic carriers of IRM and pTRM are, in fact different. As far as the IRM comprises most ferrimagnetic grains in a sample, one can guess that basically the DS of the A-state can hardly be distinguished from the DS of the B-state. Altogether, it is very likely that those

Reports... *continued on p. 8*

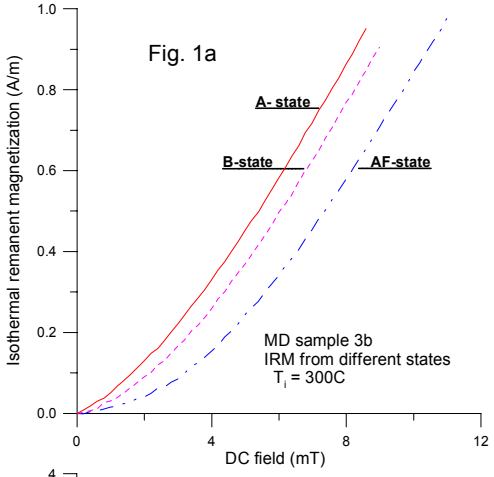

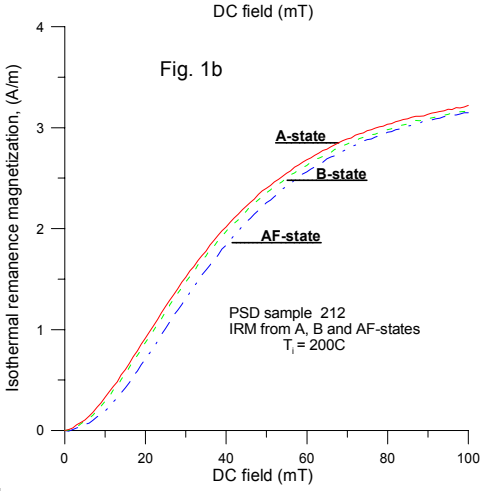

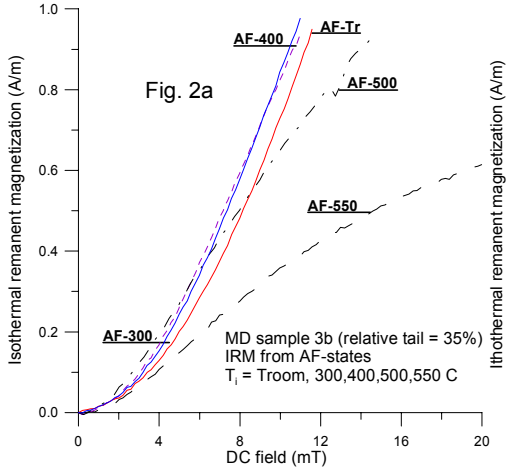

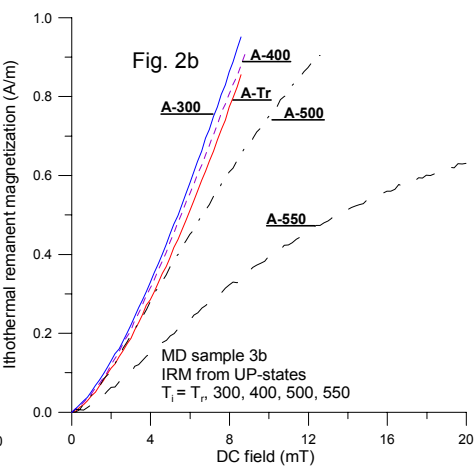

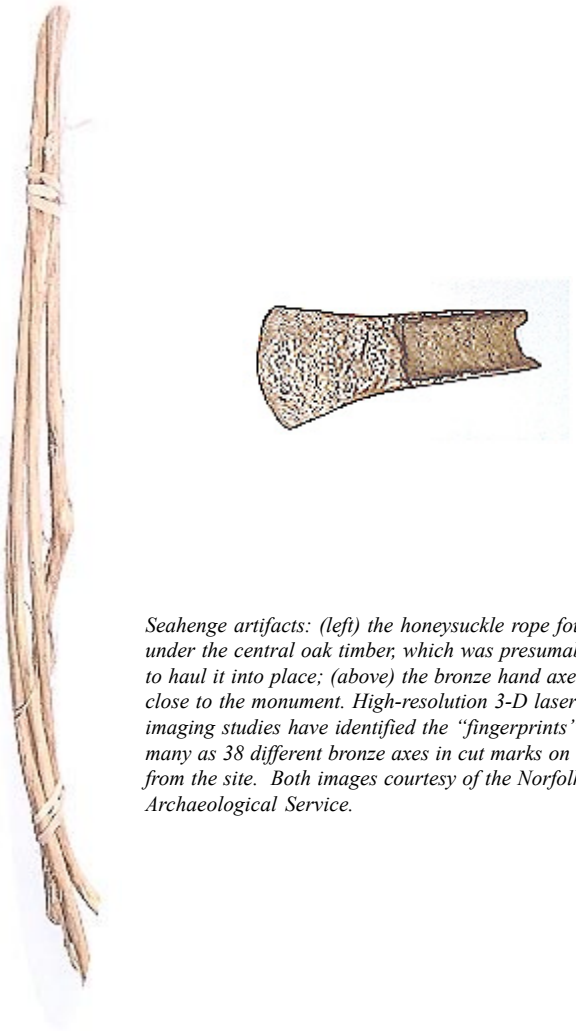

Seahenge artifacts: (left) the honeysuckle rope found under the central oak timber, which was presumably used to haul it into place; (above) the bronze hand axe found close to the monument. High-resolution 3-D laser imaging studies have identified the "fingerprints" of as many as 38 different bronze axes in cut marks on timbers from the site. Both images courtesy of the Norfolk Archaeological Service.

Current Abstracts

A list of current research articles dealing with various topics in the physics and chemistry of magnetism is a regular feature of the IRM Quarterly. *Articles published in familiar geology and geophysics journals are included; special emphasis is given to current articles from physics, chemistry, and materials-science journals. Most abstracts are culled from* INSPEC *(© Institution of Electrical Engineers),* Geophysical Abstracts in Press *(© American Geophysical Union), and* The Earth and Planetary Express *(© Elsevier Science Publishers, B.V.), after which they are subjected to Procrustean editing and condensation for this newsletter. An extensive reference list of articles (primarily about rock magnetism, the physics and chemistry of magnetism, and some paleomagnetism) is continually updated at the* IRM. *This list, with more than 5200 references, is available free of charge. Your contributions both to the list and to the Abstracts section of the* IRM Quarterly *are always welcome.*

Anisotropy

Lagroix, F., and Banerjee, S. K., 2002, **Paleowind directions from the magnetic fabric of loess profiles in central Alaska**: *Earth and Planetary Science Letters, v. 195*, no. 1-2, p. 99-112.
Two parallel loess/paleosol profiles from the Halfway House site, west of Fairbanks, span marine isotope stages 1-6 (the last ≈150 ka). AMS results show both primary eolian and secondary reworked magnetic fabrics in certain intervals of both profiles. Eolian fabrics display a horizontal magnetic foliation and a well defined magnetic lineation, corresponding to the paleodirection of sediment transport and deposition. Long-term prevailing winds appear to shift systematically from a NW-SE to N-S direction during glacial and interglacial periods, respectively.

Odah, H., Hussain, A. G., Hoffmann, V., Soffel, H. C., El-Gamili, M., and Deebes, H., 2001, **Effect of magnetic anisotropy on the experimentally determined palaeointensity of the geomagnetic field**: *Earth, Planets and Space, v. 53*, no. 5, p. 363-71.
40 samples of magnetite-bearing Nile mud were stepwise heated to 700° C in fields B_L between 0.03 mT and 0.09 mT at various angles θ. Intensities of pTRM and of total TRM increase linearly with B_L and depend on θ. In extreme cases, the anisotropy results in analog palaeointensity errors of +33% to -25%. The direction of TRM is the same as that of the ambient magnetic field independent of the anisotropy. Applying B_L in the direction of the stable NRM during a Thellier-type experiment results in accurate determination of the palaeointensity.

Anomalies & Sources

Pilkington, M., and Percival, J. A., 2001, **Relating crustal magnetization and satellite-altitude magnetic anomalies in the Ungava peninsula, northern Quebec, Canada**: *Earth and Planetary Science Letters, v. 194*, no. 1-2, p. 127-33.
A prominent satellite-altitude magnetic anomaly (>6 nT) here is coincident with a region of high-susceptibility exposed rocks. In an inversion of a combined POGO-Magsat anomaly data set, κ levels of 0.03 to 0.04 SI are required (assuming a 40-km-thick crust), well within the range of measured surface values. The Ungava peninsula is one of the few areas on Earth where a direct relation between surface rock properties and satellite magnetic anomalies can be made.

Data Analysis

Heslop, D., Dekkers, M. J., Kruiver, P. P., and van Oorschot, I. H. M., 2002, **Analysis of isothermal remanent magnetization acquisition curves using the expectation-maximization algorithm**: *Geophysical Journal International, v. 148*, no. 1, p. 58-64.
The stepwise acquisition of IRM provides an important non-destructive tool for the investigation of coercivity spectra. Through the use of an automated procedure based on the expectation-maximization algorithm, both saturated and non-saturated IRM acquisition curves can be effectively modelled into their individual coercivity contributions.

Environmental Magnetism

Brachfeld, S. A., Banerjee, S. K., Guyodo, Y., and Acton, G. D., 2002, **A 13200 year history of century to millennial-scale paleoenvironmental change magnetically recorded in the Palmer Deep, western Antarctic Peninsula**: *Earth and Planetary Science Letters, v. 194*, no. 3, p. 311-26.
Distinct shifts in glacimarine sedimentation and paleoproductivity are manifested as abrupt, order of magnitude changes in χ. The Late (3.4-0 ka) and Early Holocene (11.5-9 ka), and the Last Glacial Maximum (prior to 13.2 ka) are intervals of high χ, MD magnetite and abundant gravel grains, interpreted here as ice-rafted debris. Deglaciation (13.2-11.5 ka) and the Middle Holocene (9-3.4 ka) were times of enhanced productivity, and contain PSD magnetite and titanomagnetite, respectively. The magnetic mineral assemblage in the Deglaciation interval can be explained by density sorting in meltwater plumes. The Middle Holocene marks the onset of century-scale productivity cycles, with a magnetic mineral assemblage that suggests the reduction or cessation of locally derived terrigenous sediment.

Virina, E. I., Faustov, S. S., and Heller, F., 2001, **Implications of a paramagnetic signal for paleomagnetic studies of loess deposits**: *Izvestiya, Physics of the Solid Earth, v. 37*, no. 5, p. 423-8.
The paramagnetic signal in loess deposits is shown to have a great effect on the hysteretic characteristics, and its disregard can lead to errors in determinations of the composition and size of remanence carrier grains. In addition, the paramagnetic signal can provide constraints on landscape-climate changes in the past.

Wagner, G., Laj, C., Beer, J., Kissel, C., Muscheler, R., Masarik, J., and Synal, H. A., 2001, **Reconstruction of the paleoaccumulation rate of central Greenland during the last 75 kyr using the cosmogenic radionuclides ^{36}Cl and ^{10}Be and geomagnetic field intensity data**: *Earth and Planetary Science Letters, v. 193*, no. 3-4, p. 515-21.
The authors have derived the accumulation rate for the time interval of about 3-75 kyr BP by applying a method based on the cosmogenic radionuclides ^{36}Cl and ^{10}Be in the Summit ice cores and on geomagnetic field data. The main difference between the authors' approach and the methods applied previously is that the accumulation rate based on ^{36}Cl and ^{10}Be does not depend on an ice flow model estimating the original thickness of annual layers. The new reconstruction agrees well with the accumulation rate published by Johnsen et al. (1995) until 60 kyr BP and differs significantly from that of Cuffey and Clow (1997).

Magnetic Field Records and Paleointensity Methods

Dinares-Turell, J., Sagnotti, L., and Roberts, A. P., 2002, **Relative geomagnetic paleointensity from the Jaramillo Subchron to the**

Abstracts... *continued on p. 6*

Matuyama/Brunhes boundary as recorded in a Mediterranean piston core: *Earth and Planetary Science Letters, v. 194*, no. 3, p. 327-41.
Core LC07, located west of the Sicily Strait, records the M/B and the upper Jaramillo reversals. With an orbitally-tuned age model based on ARM/χ, the relative paleointensity minimum associated with the M/B boundary has a duration of about 4-5 kyr, while the directional change has a duration of <3 kyr. A second minimum of similar duration is found about 16 kyr below the M/B boundary. Other relative paleointensity minima are found within chron C1r.1r. In contrast to some previously published paleointensity records, spectral analysis of the LC07 record does not reveal significant power at the orbital obliquity frequency.

Morales, J., Goguitchaichvili, A., and Urrutia-Fucugauchi, J., 2001, **A rock-magnetic and paleointensity study of some Mexican volcanic lava flows during the Latest Pleistocene to the Holocene**: *Earth, Planets and Space, v. 53*, no. 9, p. 893-902.
Eleven flows sampled in the Chichinautzin volcanic field cover a geological time interval of ≈0.39 My to 2000 years. Continuous χ(T) measurements in most cases yield reasonably reversible curves with Curie points close to that of almost pure magnetite. Hysteresis ratios for all samples fall within the PSD region, probably indicating a mixture of MD and a significant amount of SD grains. 42 samples (6 cooling units) yielded acceptable absolute paleointensity estimates, with VDM values are higher than those recently reported for the past 5 My.

Shcherbakov, V. P., Shcherbakova, V. V., and Vinogradov, Y. K., 2001, **On a thermomagnetic criterion for the identification of the domain structure**: *Izvestiya, Physics of the Solid Earth, v. 37*, no. 3, p. 244-8.
The Bolshakov-Shcherbakova thermomagnetic criterion (TC) for the recognition of domain structure is based on measurement of the pTRM tail value. However, heating of a sample to T_C, required to remove its NRM, often changes the mineralogy and structure of ferromagnetic grains. An alternative to heating is AF removal of the NRM, and pTRM creation from this zero state (ZS). The TC efficiency is assessed for pTRM created from various magnetic states. The ZS-derived pTRM tail is shown to be three times smaller than its value in the standard application of TC. In the paleomagnetic practice this implies that, when ZS-derived pTRM is used, TC can provide only rough selection of multidomain samples.

Yamazaki, T., and Oda, H., 2001, **A Brunhes-Matuyama polarity transition record from anoxic sediments in the South Atlantic (Ocean Drilling Program Hole 1082C)**: *Earth, Planets and Space, v. 53*, no. 8, p. 817-27.
The cores consist of strongly anoxic sediments, deposited at rates as high as 10 cm/kyr. A continuous record of directional changes around the B/M transition was obtained from U-channel samples after AF cleaning, and confirmed using discrete samples taken from the other half of the cores. The relative paleointensity record shows following features of the B/M transition similar to those already reported by previous studies. A zone of large directional fluctuations with low paleointensities occurs just before the main transition (788 to 795 ka based on the oxygen-isotope stratigraphy), which would correspond to the "precursor" of Hartl and Tauxe (1996).

Zhong, Y., Clement, B. M., Acton, G. D., Lund, S. P., Okada, M., and Williams, T., 2001, **Records of the Cobb Mountain Subchron from the Bermuda Rise (ODP Leg 172)**: *Earth and Planetary Science Letters, v. 193*, no. 3-4, p. 303-13.
Duplicate records of the Cobb Mountain Subchron were obtained from two holes drilled in a sediment drift, and stacked to obtain a composite record. Virtual geomagnetic poles (VGPs) follow a path through the central Pacific during the lower polarity transition, very similar to VGP paths from Cobb Mountain Subchron records from other sites around the world. Furthermore, the VGPs cluster near southern Africa early in the reversal process and then group in a nearly antipodal patch in the north Pacific late in the reversal.

Zhu, R.-X., Pan, Y.-X., Shaw, J., Li, D.-M., and Li, Q., 2001, **Geomagnetic palaeointensity just prior to the Cretaceous normal superchron**: *Physics of the Earth and Planetary Interiors, v. 128*, no. 1, p. 207-22.
A new K-Ar age for the Zhuanchengzi basalt flows is 120.93±0.88 Ma. J_S-T and κ-T data show evidence of low-titanium magnetite, with a T_C of 560-585° C and generally good reversibility. Mrs/Ms and Hcr/Hc ratios indicate that PSD grains. Stepwise thermal demagnetization isolated a well-defined ChRM in all 20 flows. Reliable Thellier-Thellier palaeointensities were obtained for 42 of 71 samples. VDM values average $(3.96\pm0.07)*10^{22}$ Am^2, approximately half the present day VDM, indicating a weak geomagnetic field just prior to the CNS.

Magnetic Microscopy and Spectroscopy

Novikov, S. I., Lebedeva, E. M., Schtoltz, A. K., Yurchenko, L. I., Tsurin, V. A., and Barinov, V. A., 2002, **Distribution of cations in magnetite prepared by mechanochemical synthesis**: *Physics of The Solid State, v. 44*, no. 1, p. 124-32.
The distribution of iron cations in the crystal lattice of the $Fe_{3-\delta}O_4$ (δ = 0.153) cation-deficient spinel is investigated using XRD and Mössbauer spectroscopy. Analysis of the Mössbauer data shows that the $Fe_{2.847}O_4$ magnetite prepared by mechanochemical synthesis is a chemically heterogeneous compound. The crystal structure of $Fe_{2.847}O_4$ is characterized by local environments of the ($Fe^{2.5+}$) cations at $\delta_0 \leq 0.1$, δ_1 equivalent to 0.12, δ_2 equivalent to 0.18, and δ_3 equivalent to 0.26, which are responsible for a broad distribution of magnetic hyperfine fields with the P(H) probability maxima near 37.0, 36.0, 34.0, and 30.0 MAm^{-1}.

Pan, Q., Pokhil, T. G., and Moskowitz, B. M., 2002, **Domain structures in epitaxial (110) Fe_3O_4 particles studied by magnetic force microscopy**: *Journal of Applied Physics, v. 91*, no. 9, p. 5945-50.
Patterned particles ranging in size from 2x2 to 10x10 μm were prepared from 250-nm thick magnetite films grown on MgO. The particles showed in-plane, stripe-like domain structures with ill-defined walls mainly along the in-plane [110] direction. Individual wall sections were highly fragmented with variable widths (100-300 nm) and subdivided into opposite polarity segments of variable lengths. The unusual domain wall structures are a consequence of antiferromagnetically coupled, growth-induced, structural antiphase domains and antiphase boundaries (APB). Analysis of the domain spacing as a function of particle size yields an estimate of the average exchange stiffness constant that is nearly 2 orders of magnitude lower than the value in bulk magnetite, consistent with the idea that exchange interactions across the APBs are severely suppressed due to spin frustration.

Wright, J. P., Attfield, J. P., and Radaelli, P. G., 2001, **Long range charge ordering in magnetite below the Verwey transition**: *Physical Review Letters, v. 87*, no. 26, p. 266401/1-4.
The crystal structure of Fe_3O_4 below the 122 K Verwey transition has been refined using high-resolution x-ray and neutron powder diffraction data. The refinements give direct evidence for charge ordering (CO) over four independent octahedral Fe sites, two with a charge of +2.4 and the other two of +2.6. CO schemes consistent with our model do not meet the widely accepted Anderson condition of minimum electrostatic repulsion. Instead we propose that CO is driven primarily by a [001] electronic instability, which opens a gap at the transition through a charge density wave mechanism.

Magnetization Processes

Bazhenov, M. L., and Mikolaichuk, A. V., 2002, **Paleomagnetism of Paleogene basalts from the Tien Shan, Kyrgyzstan: rigid Eurasia and dipole geomagnetic field**: *Earth and Planetary Science Letters, v. 195*, no. 1-2, p. 155-66.
Only a single-component remanence of reversed polarity is present in these basalts above 200-260° C. The overall mean direction of this remanence agrees well with the Eurasian reference directions for the Paleogene, in sharp contrast with most earlier published Cenozoic inclinations from Central Asia which are 20-30° shallower than the expected values. Good agreement of the reference inclinations and those from basalts rules out models which invoke non-dipole fields and/or large-scale tectonic motions for explanation of the Cenozoic inclination anomaly. Instead, a mechanism related to NRM acquisition in redbeds is strongly indicated.

Gilder, S., Chen, Y., and Sevket, S., 2001, **Oligo-Miocene magnetostratigraphy and rock magnetism of the Xishuigou section, Subei (Gansu Province, western China) and implications for shallow inclinations in**

abstracts... *continued on p. 7*

central Asia: *Journal of Geophysical Research, v. 106*, no. B12, p. 30505-21.
Magnetostratigraphy and paleontology suggest that 2179 m of this were deposited from 26 to 19 Ma. Stratigraphic patterns of χ, AMS, NRM and ARM intensities demonstrate that (1) faulting does not significantly affect the record, (2) sediment deposition was relatively continuous, (3) sediment source changed around 23 Ma, and (4) rapid uplift occurred at 21 Ma. The paleolatitude of Subei is 19° ±3° less than predicted from the reference pole. Both rock magnetic and paleomagnetic data sets suggest that the unusually low paleolatitude is the result of synsedimentary inclination shallowing, a phenomenon which has likely affected other paleomagnetic data from central Asia.

Jordanova, D., Yancheva, G., and Gigov, V., 2001, **Viscous magnetization of loess/ palaeosol samples from Bulgaria**: *Earth, Planets and Space, v. 53*, no. 3, p. 169-80.
VRM acquisition in three sets of palaeosol and loess samples are linear functions of log t for 10 min. to 30 day experiments. Linear correlation of the acquisition coefficients, normalized to M_S, with the ratio χ/M_S suggests that mainly SP/SSD grains are involved. VRM decay is non-linear with log t, especially for the first 10 min. of the experiment. This phenomena is explained in terms of of composite grains (core/shell structure), formed as a result of low-temperature oxidation.

Mineral & Rock Magnetism

Alva-Valdivia, L. M., Goguitchaichvili, A., Urrutia-Fucugauchi, J., Caballero-Miranda, C., and Vivallo, W., 2001, **Rock-magnetism and ore microscopy of the magnetite-apatite ore deposit from Cerro de Mercado, Mexice**: *Earth, Planets and Space, v. 53*, no. 3, p. 181-92.
CRM seems to be present in most of the ore and wall rock samples, replacing an original TRM. Magnetite (or Ti-poor TM) and hematite are commonly found in the ores. Although hematite may carry a stable CRM, no secondary components are detected above 580°. Reflected light microscopy shows that the magnetic carriers are mainly titanomagnetite, with significant amounts of ilmenite-hematite minerals, and goethite-limonite resulting from alteration processes. Magmatic titanomagnetites, which are found in igneous rocks, show trellis, sandwich, and composite textures, which are compatible with high temperature (deuteric) oxy-exsolution processes.

Bazhenova, G. N., Genshaft, Y. S., Pechersky, D. M., and Sharonova, Z. V., 2001, **Petromagnetic characteristics and ore minerals of crystalline rocks in the Aldan-Stanovoi ring structure**: *Izvestiya, Physics of the Solid Earth, v. 37*, no. 5, p. 402-13.
Ores are represented by isolated, rather large grains (a few tens to a few hundreds of micrometres) of ilmenite and magnetite and, more often, by their intergrowths. Magnetic characteristics of the rocks are mainly controlled by magnetite produced during subsolidus transformations of primary magmatic oxide phases represented by titanomagnetite and hemoilmenite. The decomposition structures of solid solutions of these phases are well developed. The magnetite concentrations estimated from magnetic data are less than 0.1 to 13 vol %. The magnetization of the samples virtually does not depend on the extent and type of secondary alterations of the rocks and on their fabric state.

Kletetschka, G., and Wasilewski, P. J., 2002, **Grain size limit for SD hematite**: *Physics of the Earth and Planetary Interiors, v. 129*, no. 1-2, p. 173-9.
The SD- MD transition for hematite occurs at 0.1 mm, as shown by the size dependence of H_C and χ, and an anomaly in remanence recovery when cycling through the Morin transition. For grains larger than 0.1 mm χ depends on the amplitude of the applied ac field. This behavior is ascribed to a transition from the metastable SD to the MD state. The 0.1 mm transition has no significant effect on shape of the temperature-dependent coercivity and saturation magnetization.

Kosterov, A., 2001, **Magnetic properties of subaerial basalts at low temperatures**: *Earth, Planets and Space, v. 53*, no. 9, p. 883-92.
In 21 subaerial basalt samples of different origin and age, low-Ti TM is the dominant NRM carrier. New measurements from 2-300 K indicate the presence of another magnetic mineral in all samples, which accounts for up to 70% of M_S at 2 K and acquires a strong low-T SIRM. χ(T) curves measured in different DC fields show peaks, marking the effective T_B, that shift from <2 K to about 16 K in a 4.8 T DC magnetic field. A possible candidate to account for these properties is a hemoilmenite with 8-10 mole% of hematite, originating from high-temperature deuteric oxidation.

McEnroe, S. A., Harrison, R. J., Robinson, P., Golla, U., and Jercinovic, M. J., 2001, **Effect of fine-scale microstructures in titanohematite on the acquisition and stability of natural remanent magnetization in granulite facies metamorphic rocks, southwest Sweden: implications for crustal magnetism**: *Journal of Geophysical Research, v. 106*, no. B12, p. 30523-46.
These granulites contain hematite-ilmenite with minor magnetite, and occur in an area with negative aeromagnetic anomalies. Samples were characterized by optical microscopy, electron microprobe, TEM, and rock-magnetic measurements. Earliest oxide equilibrium was between grains of titanohematite and ferri-ilmenite at 650°-600° C. Initial contacts were modified by many exsolution cycles. TEM microstructures consist of gently curving semicoherent ilmenite lamellae within hematite, flanked by precipitate-free zones and abundant ilmenite disks down to unit cell scale (1-2 nm). Intensity of magnetization is greater than possible with hematite alone, and TEM work suggests that ultrafine R3 ilmenite disks in AF hematite are associated with a ferrimagnetic moment due to local imbalance of up and down spins at coherent interfaces.

Özdemir, O., Dunlop, D. J., and Moskowitz, B. M., 2002, **Changes in remanence, coercivity and domain state at low temperature in magnetite**: *Earth and Planetary Science Letters, v. 194*, no. 3, p. 343-58.
Magnetite crystals with a mean size of 0.037 μm are SD both in the cubic phase at room temperature T_0 and in the monoclinic phase below the Verwey transition (T_v≈120 K). The 0.10 and 0.22 μm crystals have a mixture of SD and 2D states at T_0, but mainly SD structures below T_v. Hc increases on cooling through T_v, by a factor 3-5 in the submicron magnetites and 40 in a 1.3 mm single crystal. SIRM produced at 5 K drops by 70-100% in warming across T_v, with minor recovery in cooling back through T_v. In contrast, SIRM produced in the cubic phase at 300 K decreases 5-35% (submicron) or >95% (1.3 mm) during cooling from 300 to 120 K due to continuous re-equilibration of domain walls, but there is little further change in cooling through T_v itself. The submicron magnetites lose a further 5-15% of their remanence when reheated through T_v. The irreversibility is mainly caused by 2D to SD transformations on cooling through T_v, which preserve or enhance remanence, while SD to 2D transformations on warming through T_v cause remanence to demagnetize.

Smirnov, A. V., and Tarduno, J. A., 2002, **Magnetic field control of the low-temperature magnetic properties of stoichiometric and cation-deficient magnetite**: *Earth and Planetary Science Letters, v. 194*, no. 3, p. 359-68.
The authors report three types of low-T (< 120 K) magnetic behavior from oxidized and stoichiometric PSD magnetite: (1) a non-monotonic dependence of the M_{RS}/M_S ratio on the magnetic field (0-1.7 T) applied during cooling, (2) an induced magnetic anisotropy at temperatures below the 120 K Verwey transition after cooling in magnetic fields between 0.01 and 0.09 T, and (3) a non-monotonic dependence of a low-T (10 K) remanent magnetization on the magnetic field (0.01-2.5 T range) applied during cooling through T_V. These phenomena are interpreted in terms of relationships between crystal twins, that can form in monoclinic magnetite, and the reorganization of magnetic domains.

Worm, H. U., 2001, **Magnetic stability of oceanic gabbros from ODP Hole 735B**: *Earth and Planetary Science Letters, v. 193*, no. 3-4, p. 287-302.
These gabbros have a very stable NRM of reversed polarity with most T_{UB}s slightly below the T_C of magnetite. The demagnetization data yield only a very small secondary component acquired during the Brunhes or an earlier normal chron, suggesting a strong resistance against the acquisition of VRM. A novel furnace has been designed for measurements at high temperatures inside a commercial SQUID magnetometer, and magnetic viscosity experiments have been conducted on the gabbros up to 550° C. The alteration of the magneto-mineralogy is interpreted to result from the annealing of defects in magnetite that originate from tectonically induced strain. The oceanic gabbros of Hole 735B are thus ideal source layer material for marine magnetic anomalies, and secondary VRM acquisition, as a possible

Abstracts... *continued on p. 8*

cause for anomalous skewness, is essentially absent.

Modeling and Theory

Aharoni, A., 2001, **Micromagnetics: Past, present and future**: *Physica B, v. 306*, no. 1, p. 1-9.
The theory of micromagnetics started with great hopes of describing rigorously all magnetization process in ferromagnets. This goal has never been achieved, or even approached, for several reasons. Some of the reasons are misinterpretations and mistakes, introduced by those who misunderstood the whole theoretical approach. These mistakes must be removed and corrected. Others may be inherent to the physical limitations of the theory, but they can be removed by some modification and generalization of the basic assumptions. The ways to proceed, and the directions that micromagnetics should take in the future, are listed here, based on extrapolating from its history.

Horng-Tay, J., and Guo, G. Y., 2002, **First-principles investigations of the electronic structure and magnetocrystalline anisotropy in strained magnetite Fe_3O_4**: *Physical Review B, v. 65*, no. 9, p. 094429/1-9.
The electronic structure and magnetocrystalline anisotropy energy have been calculated for fcc Fe_3O_4 under uniaxial strain applied along the [001] direction. The calculated fourth-order anisotropy constant K_1 is in fair agreement with the experimental value. The magnitude of K_1 appears to be suppressed under large extensive lateral strains. The second order uniaxial anisotropy constant K_{out} is positive for extensive in-plane strains and is negative for compressive in-plane strains. The positive value of K_{out} minus the shape anisotropy indicates that an Fe_3O_4 film under an extensive in-plane strain larger than 0.2% would show perpendicular magnetization, in good agreement with recent experiments on Fe_3O_4 films on MgO(100) and CoO(100).

Seo, H., Ogata, M., and Fukuyama, H., 2002, **Aspects of the Verwey transition in magnetite**: *Physical Review B, v. 65*, no. 8, p. 085107/1-9.
Mean-field calculations for a three-band model of spinless fermions, appropriate for d electrons of Fe ions in B sites, indicate that the phase transition should be a bond dimerization, due to the cooperative effects of strong electronic correlation and electron-phonon interaction. The results show that the ferro-orbital ordered state is stabilized in a wide temperature range due to the strong on-site Coulomb interaction between different t_2g orbitals, resulting in an effectively one-dimensional electronic state, which leads the system toward an insulating state through a Peierls lattice distortion with a period of two Fe(B) ions, i.e., bond dimerization. Furthermore, it is found that the interplay between such lattice distortions in Fe(B) ions, and the lattice elastic energy of Fe(B)-O as well as Fe(A)-O bonds, gives rise to a competition between two different three-dimensional patterns for the bond dimerization, and can stabilize a complicated one with a large unit-cell size.

Shcherbakov, V. P., and Sycheva, N. K., 2001, **Numerical modeling of the domain structure in magnetite grains of submicron sizes**: *Izvestiya, Physics of the Solid Earth, v. 37*, no. 4, p. 334-44.
Only a uniform SD structure exists at d≤50 nm. In cubic magnetite particles, at least two modes coexist at d=55.5-110 nm: a PSD "flower" mode and a "curling" mode. The upper limit of the flower mode existence is 110 nm. The curling mode prevails (with its configuration being somewhat complicated) throughout the interval d=55.5-500 nm considered in this paper and has the lowest energy and the highest stability. Accordingly, the flower mode is metastable nearly throughout the region of its existence d=50-110 nm. In magnetite particles having the shape of an oblong ellipsoid of revolution, the SD structure is transformed directly into the curling mode, ignoring the flower mode. The critical size of this transition for a sphere is 53.5 nm. At a ratio of the ellipsoid axes of 3.17, the grain is in a stable SD state regardless of its size.

Synthesis and Properties of Magnetic Materials

Narasimhan, B. R. V., Prabhakar, S., Manohar, P., and Gnanam, F. D., 2002, **Synthesis of gamma ferric oxide by direct thermal decomposition of ferrous carbonate**: *Materials Letters, v. 52*, no. 4, p. 295-300.
Ferrous carbonate was precipitated from the reaction of ferrous sulfate and sodium carbonate in an aqueous medium. The precipitate was calcined at different heating rates (2, 5 and 10° C/min, respectively) up to 500° C and the iron oxides produced were found to be magnetic. X-ray diffraction studies indicated the presence of gamma ferric oxide as a major phase in all the cases. It was found that wet precipitates, faster heating rate and short residence time in the furnace produced gamma ferric oxides with better magnetic properties (coercivity of around 360 Oe and saturation magnetization of 64 emu/g). The effect of aging time of ferrous carbonate precipitates on the magnetic properties was also studied.

Yamaguchi, I., Terayama, T., Manabe, T., Tsuchiya, T., Sohma, M., Kumagai, T., and Mizuta, S., 2002, **Preparation of (111)-oriented epitaxial Fe_3-xO_4 films on α-Al_2O_3(0001) substrates by coating-pyrolysis process using postepitaxial topotaxy via (0001)-oriented α-Fe_2O_3**: *Journal of Solid State Chemistry, v. 163*, no. 1, p. 239-47.
We have prepared (111)-oriented epitaxial films of magnetite (Fe_3O_4) and maghemite (γ-Fe_2O_3), or Fe_3-xO_4, on the C-planes of sapphire [α-Al_2O_3(0001)] by a coating-pyrolysis (CP) process using postepitaxial topotaxy (PET). The PET process consists of one epitaxial growth and one or more topotactic reaction steps. A (0001)-oriented epitaxial film of hematite was first formed on an α-Al_2O_3(0001) substrate by CP. Second, α-Fe_2O_3 was reduced to Fe_3O_4 in an argon-hydrogen gas flow. Finally, the Fe_3O_4 was oxidized in air to γ-Fe_2O_3, or $Fe_{3-x}O_4$. Pole-figure analysis exhibited that both the products, Fe_3O_4 and γ-Fe_2O_3, were (111)-oriented and epitaxially grown on the substrate surface. This implies that α-Fe_2O_3 (0001) has been topotactically converted to Fe_3O_4 (111) and γ-Fe_2O_3 (111).

Xu, X. N., Wolfus, Y., Shaulov, A., Yeshurun, Y., Felner, I., Nowik, I., Koltypin, Y., and Gedanken, A., 2002, **Annealing study of Fe_2O_3 nanoparticles: Magnetic size effects and phase transformations**: *Journal of Applied Physics, v. 91*, no. 7, p. 4611-16.
Sonochemically synthesized Fe_2O_3 nanoparticles were annealed in air or in vacuum while their magnetization was continuously recorded. Annealing in vacuum at temperatures T_A between 240 and 450° C produced nanophases of γ-Fe_2O_3 with average particle size ranging from 4 to 14 nm, depending on T_A. Phase transformation into α-Fe_2O_3 occurred directly by annealing in air, or via an intermediate Fe_3O_4 phase by annealing in vacuum at T_A>450° C. Mapping the correlation between the magnetic properties and the annealing conditions, enables control of the annealing process to obtain nanocrystals of γ-Fe_2O_3, α-Fe_2O_3, or Fe_3O_4 with different particle size and magnetic properties.

...Reports
continued from p. 4

parts of the DS of a grain which respond to the thermofluctuations (and, hence, closely relates to the pTRM carriers) do differ. However, they obviously occupy only a small fraction of the total grain volume, which makes it extremely difficult to spot such the patterns.

One might envy IRM collection of modern magnetometric devices but the point is that the IRM staff is commited to share this abundance with their visitors. I greatly thank all of them for their kind, sincere and omnipresent help, not to mention the valuable scientific and non-scientific discussions.

References

Shcherbakov, V.P., McClelland E. & Shcherbakova, V.V., A model of multidomain thermoremanent magnetization incorporating temperature-variable domain structure. *J. Geophys. Res*., **98**, 6201-6216, 1993.

Shcherbakova, V.V., V.P. Shcherbakov, F. Heider, Properties of partial thermoremanent magnetization in PSD and MD magnetite grains. *J. Geophys. Res*, **105**, B1, pp. 767-782, 2000.

V. P. Shcherbakov, V. V. Shcherbakova, Y. K. Vinogradov and F. Heider "Thermal stability of pTRMs created from different magnetic states, *PEPI*, **126**, pp. 59-73, 2001.

...Seahenge

continued from p. 1

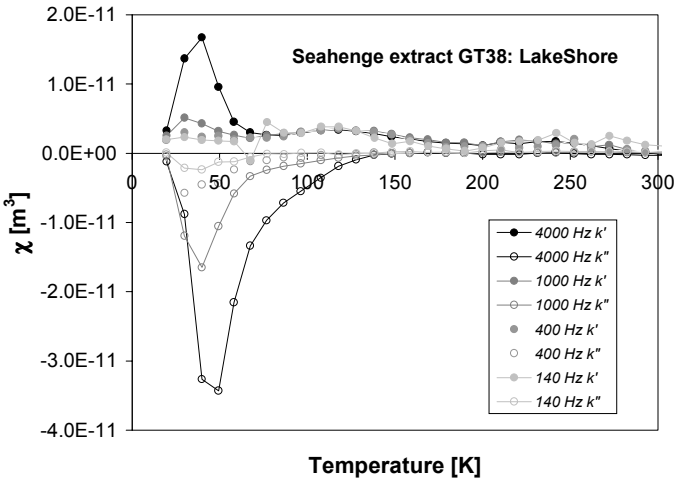

Fig. 2 In-phase (χ') and quadrature (χ") susceptibilities for a Seahenge extract (>38 μm), as functions of temperature and frequency, measured using the Lakeshore susceptometer.

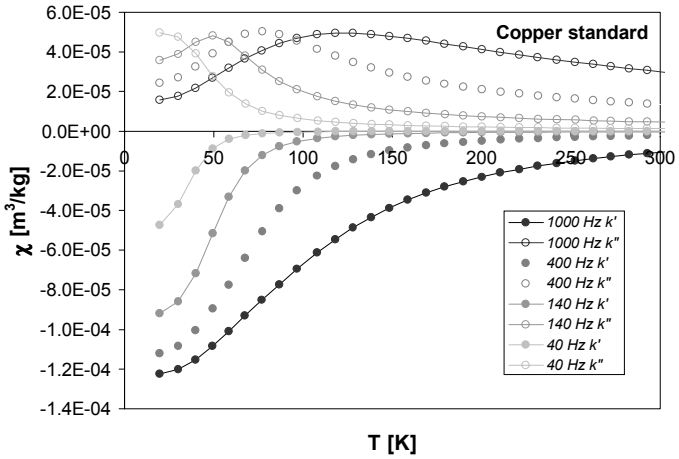

Fig. 3 In-phase (χ') and quadrature (χ") susceptibilities for a cylindrical copper standard, as functions of temperature and frequency, measured using the Lakeshore susceptometer.

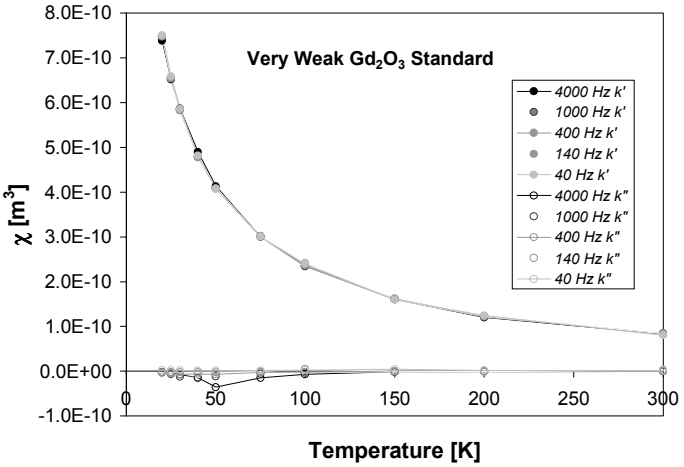

Fig. 4 In-phase (χ') and quadrature (χ") susceptibilities for a "very weak" gadolinium oxide standard, as functions of temperature and frequency, measured using the Lakeshore susceptometer.

minerals in the sediment.

Further investigation of the Seahenge samples therefore seemed warranted including the preparation of magnetic extracts to help precisely nail down the magnetic minerals responsible through low temperature measurements. What could be more straightforward?

Anomalous Low-T AC Susceptibility

Among the various measurements made to characterize magnetic mineralogy and size distributions, probably the best for distinguishing the superparamagnetic fraction is frequency-dependent susceptibility χ(f) at low temperatures (20-300K). However, a set of rather bewildering results (Fig 2) obtained from the recently-reconstructed Lakeshore susceptometer did not suggest any obvious interpretation in terms of superparamagnetism or mineralogy, although it did seem to indicate something exceptional about these specimens[(1)]. The frequency-dependence of χ' is strongly negative near 50 K (i.e., χ' *increases* with f), and there is a large negative peak in χ" in the same temperature range. Readers familiar with the AC response of conductive materials [*e.g., Worm et al.*, 1993; *Wait*, 1951] will recognize the increase in the magnitudes of both χ' and χ" with frequency asa conductive response, in this case restricted to temperatures near 50 K. Discerning readers will also note, however, that the signs are "wrong": conductive (and weakly magnetic) samples should have χ'<0 and χ">0 [*ibid*].

For example, the same experiment run on a cylindrical specimen of pure copper produced the results shown in Fig 3. These data can be modeled quite accurately using equation 1 of *Worm et al.* [1993], with a conductivity that increases smoothly on cooling, from ~$6x10^7$ S/m (exactly equal to the "book" value [*CRC*, 1974]) at 300 K to ~$5x10^9$ S/m at 20 K. Note that the magnitude of χ' increases monotonically with frequency at all temperatures, whereas χ" is a non-monotonic function of frequency at low temperatures. The data for the Seahenge extract exhibit a similar sort of frequency-dependence, albeit restricted to a narrow temperature interval, suggesting that something in the sample becomes highly conductive at those temperatures[(2)]. No other mechanism that we are aware of generates an apparent susceptibility signal that increases with frequency. However, the "wrong" sign is troublesome.

Such singular results beg the question: are we seeing the results of some sort of instrumental artifact, or learning something significant about the specimen (or perhaps both?). During the excarnation and complete reconstruction necessitated by its gruesome meltdown (see *Quarterly v.8 n.4*), the Lakeshore was equipped with a new preamplifier, boosting the signal/noise ratio significantly and enabling measurement of samples that had previously been too weak. Calibration and testing, using various paramagnetic standards of different strengths, had not uncovered any problems[(3)] (Fig 4), but behavior as exotic as that in Fig 2 demands some confirmation, so we measured the same sample again using the Quantum Designs MPMS, with the results shown in Fig 5.

Although the results look decisively different (and thus appear to incriminate the Lakeshore), in fact the ambiguity is nearly perfect, owing to the different frequency ranges of the two instruments (the Lakeshore range extends nominally down to 10 Hz, but for weak samples the effective lower limit is about 100 Hz; for the MPMS the *upper* limits are 1000 and 10 Hz, respectively). Thus the question remains: are the Lakeshore results dominated by specimen properties, instrumental artifacts, or some combination thereof?

Closer scrutiny of the calibration run in Fig 4 suggests that the innocuous-looking glitch in χ" near 50 K may be more nocuous than it originally seemed. Note that although its magnitude is very small in comparison to χ' for this weakest standard, it is in fact quite close to the magnitude of the χ" signal for the Seahenge extract (~$3.5x10^{-11}$ m^3, Fig 2). The next obvious test was a "blank" measurement of an empty gelcap under the same conditions. (Blank runs are standard for background and/or noise-level characterization on most *IRM* instruments. However with the Lakeshore, one of the most reliable features of the software is a bug that makes it crash with very low signal levels, and therefore blank runs have not been part of the standard repertoire for this instrument). The results of a blank run are shown, in effect, in Fig 2 (alas). All of the major features in Fig 2, and even some minor ones (such as the broad minor peak in χ' near 120 K) are duplicated with merciless precision in the blank run. This Seahenge extract is extraordinarily weakly magnetic, but beyond that the Lakeshore data provide scant characterization.

Why Does It Do That?

Although irrelevant to the Seahenge study, it is of interest to consider the cause of the Lakeshore's low-temperature self-excitation. The immediate prime

[(1-N)] For clarity & convenience, some good ways to be wrong are indicated by sequential superscripting.

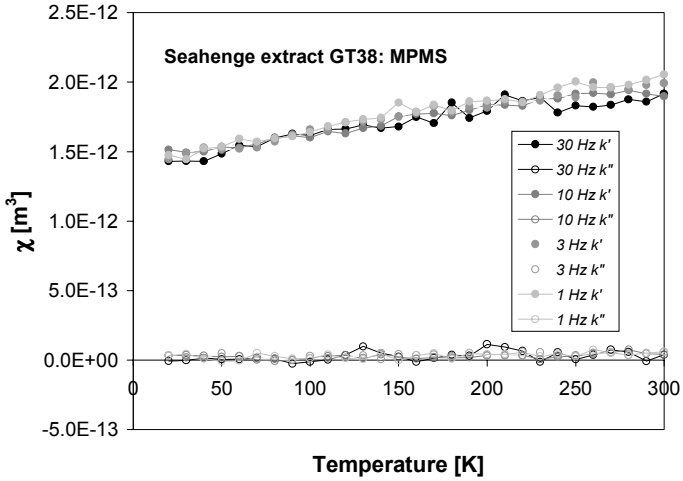

Fig. 5 In-phase (χ') and quadrature (χ") susceptibilities for a Seahenge extract (>38 μm), as functions of temperature and frequency, measured using he MPMS.

suspect was the brass rod from which the samples are suspended (Fig 6). At room temperature, brass is quite conductive (15-25% as much as copper [*CRC*, 1974]), but the cause of the observed variations with temperature (Fig 2) is unclear. The sign reversal can be understood in terms of the coil/sample/holder geometry, shown in Fig 6. The inner solenoidal sensing coils are wired in series and oppositely-wound, in order to cancel out the voltages induced in each (Lenz's law) by the sinusoidally-time-varying primary field, which is applied by the long outer solenoid. The net voltage when a sample is positioned in either sensing coil is proportional to the secondary field produced by the sample, i.e., proportional to sample susceptibility and volume. Each measurement involves a pair of readings, one (V_1) with the sample in the lower (negative) coil and one (V_2) in the upper (positive) coil, followed by appropriate averaging ($<V> = [V_2-V_1]/2$). A transport mechanism at the upper end positions the sample by moving the brass rod up or down. Due to the geometry and mode of measurement, any secondary fields generated by conductive eddy currents in the brass rod are sensed by the pickups: (a) more strongly in the upper (+) coil than in the lower (-), so both V_1 and V_2 are positive; and (b) most strongly when the sample is positioned in the lower coil, so that $|V_1| > |V_2|$. Hence any conductive signal from the brass would be detected with the "wrong" sign.

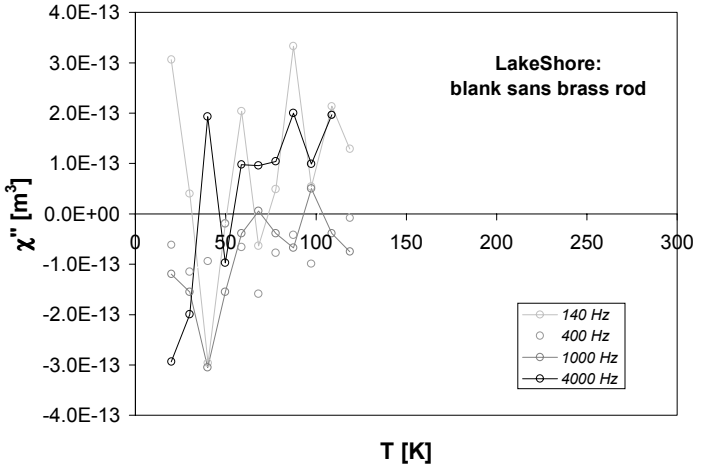

Fig. 7. Quadrature susceptibility for a blank run on the Lakeshore susceptometer, in which the entire sample rod/holder assembly was kept out of the instrument.

Further blank runs, omitting both sample and brass rod, all failed to complete execution due to the previously-mentioned software bug. However one run persisted to 120K (Fig 7), and showed clearly that the anomaly disappeared in the absence of the brass rod, proving its guilt beyond reasonable doubt[4]. Imagine our surprise, then, when the 50 K anomaly reappeared, essentially unaltered, after replacing the brass rod with a newly-engineered carbon-fiber replacement! It seems impossibly unlikely that both materials would have strong conductivity anomalies in the same temperature range. Moreover, direct measurements on a piece of the brass rod, properly centered in the sensing coils, showed only small and gradual changes in conductivity with temperature. If the brass rod was not the source of the anomalous behavior, then what was?

One thing that remained unchanged in the brass->carbon replacement was the plug of kapton tape at the end of the rod, to which the sample/straw assembly is attached (Fig 6). Inescapably, then, this *must* be the culprit[5]. The obvious test of measuring the tape plug directly, however, seems to prove its innocence: the tape has negligible conductivity (as well as negligible susceptibility) over the whole temperature range.

We are therefore left with a bedeviling conundrum. The 50 K anomaly cannot be produced directly by any of the materials used in the sample holder/rod assembly, yet the anomaly disappears when this assembly is not present! It seems that the only escape from this paradox is to call upon some sort of indirect or compound mechanism, e.g., a chain of flux linkages in which the rod assembly plays just one part.

The restricted temperature range of the aberrant behavior also remains an interesting puzzle. Sharp variations in electrical, magnetic and thermal properties are often associated with phase transitions, and it still seems likely that some such phenomenon is involved in producing the observed anomalies. For example, oxygen might be considered a suspect, since it has two significant transitions that nearly bracket the temperature range of the anomalous behavior: the β-γ antiferromagnetic-paramagnetic transition at about 42 K [Gregory, 1978], and the solid-liquid transition near 54 K. However, the oxygen concentration in the system

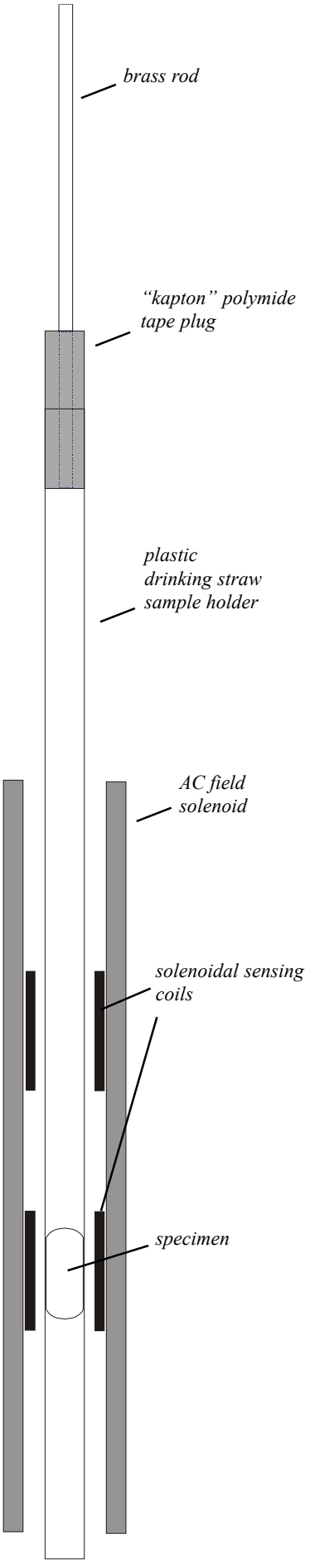

Fig 6. Sample/coil geometry in the Lakeshore susceptometer (actual size).

Lenz, Heinrich

b. Feb 12, 1804, Tartu (Dorpat), Estonia
d. Feb 10, 1865, Rome

After completing his doctorate at the age of 20, Lenz accompanied Otto Kotzebue on the latter's second voyage of circumnavigation (1823-6), serving as naturalist. His observations were published after his return by the Academy of Sciences at St Petersburg, to which he was soon elected as a member. He became professor of physics at the University there, and worked on electrical conduction, establishing the quadratic dependence of resistivity upon temperature for metals. Like his slightly-older contemporaries Faraday and Henry, Lenz is remembered primarily for his ground-breaking original contributions to the study of electromagnetic induction. Lenz's Law was introduced in his 1833 presentation to the Academy "On the Direction of Galvanic Currents Which Are Excited through Electrodynamic Induction."

...Seahenge
continued from p. 9

should be vanishingly small. The instrument is thoroughly evacuated and flushed with helium repeatedly prior to cooling.

We are continuing to work on understanding and rectifying the anomalous behavior. Minimizing the volume of sample rod material, and maximizing its separation from the sample, have decreased the anomaly amplitude substantially ($|\chi''|_{max} \sim 5 \times 10^{-12}$ m^3). In general the problem is of more academic than practical interest, since (a) the magnitude of the anomaly is small enough that it is negligible in all but the weakest samples, and (b) it is quite reproducible, and a "background subtraction" can often largely eliminate the anomaly from measured data.

Close scrutiny of some older data shows that this self-excitation occurred before the re-engineering of the Lakeshore, but it was mostly buried safely within the instrument noise level. Despite the Seahenge-like emergence of this anomalous behavior, the Lakeshore is clearly a better instrument now than it has ever been.

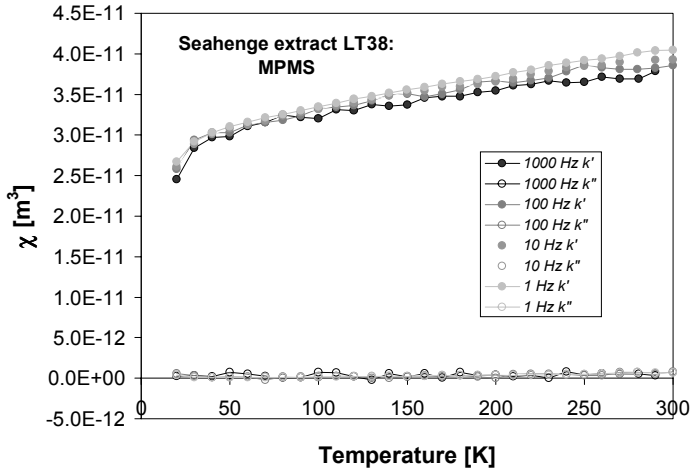

Fig. 8 In-phase (χ') and quadrature (χ") susceptibilities for a Seahenge extract (<38 μm), as functions of temperature and frequency, measured using the MPMS.

Archaeological Upshot

Bedeviling instrumental conundrums aside, the archaeological interpretation of all this data proved something of a roller coaster ride. The impact of the initial results was stunning and provided irrevocable proof for those searching for evidence to support the theory of extraterrestrial intervention to explain the technological ascent of prehistoric culture. We had obviously discovered a highly exotic, low-temperature superconducting material clearly associated with the remains of the Seahenge. Far from being a primitive ritual monument, the timber circle appeared to be the core around which a giant superconducting solenoid was formed*. This coil would, no doubt, have been used to propel space capsules from the central oak stump beyond the gravitational field of the earth! Experiments performed with an accurate scale model of the Seahenge site (ASC Pulse Magnetiser and rare earth spherical magnetic projectiles) appeared to fully support the practicality of this novel proposal, producing escape velocities that could easily clear the width of the IRM laboratory (B. Carter-Stiglitz *pers comm*).

Alas, how the reality of the Lakeshore results pulled our novel interpretation back down to earth. It seems, on balance, that a more sober interpretation of the Seahenge magnetic enhancement is due to the presence of iron sulphides, probably a mixture of greigite and pyrrhotite (the latter perhaps accounting for the slight increase in χ' at 30K found in the MPMS data for the fine fraction of the extract (Fig 8)). The quasi-linear increase of χ' with temperature above 30K, together with the *positive* frequency-dependence, suggest a contribution from a superparamagnetic population with a lognormal size distribution [*Worm*, 1998]. A diagenetic origin unrelated to either the construction process or use of the monument therefore seems the most likely explanation.

Turning full circle

The decision by English Heritage to fully excavate the Seahenge site was not taken lightly but, in this case, the preferred option of preservation *in situ* seemed unrealistic given the rapid denudation of sand and silt from the beach. Whilst the shifting sands on this part of the Norfolk coastline often provide brief glimpses of the past before shrouding them again with silt, the potential damage that might have occurred to the exposed timbers was considered too great a risk. Opinion was certainly divided during the excavation and this proceeded with frequent interruption from protestors who felt the sanctity of the monument would be best preserved by leaving the site in peace.

However, the excavation did afford an opportunity to study the monument in much greater detail, including laser scanning of cut marks made on the timbers by Bronze tools during the construction of the circle. Whilst the Bronze age axe found in the vicinity of Seahenge is actually thought to be 500 years younger than the circle itself, evidence for over 38 individual metal tools was found through the laser scanning. Given that metal working technology was only introduced from the continent approximately 100 years before the construction of Seahenge, the enormous importance of the monument to its builders and the social cohesion this implies sheds a fascinating light on the workings of Bronze age society.

Currently, the Seahenge timbers are being fully conserved by gradually replacing the salt water at the Flag Fen Bronze Age centre. This process may take several years to achieve but will ensure the survival of an unique monument, hopefully reconstructed in a museum or visitors centre, for at least another 2 millennia.

References

Bayliss, A., Groves, C., McGormac, G., Baillie, M., Brown, D. and Brennand, M., (2000). Precise dating of the Norfolk timber circle. *Nature,* **402**, pp479.

CRC Handbook of Chemistry and Physics, 55th edition, R. C. Weast, ed., CRC Press, Cleveland.

Gregory, S., (1978). Magnetic susceptibility of oxygen adsorbed on graphite. *Physical Review Letters*, **40**, no.11, pp.723-5.

Linford, N. T., (1999). Visiting Fellows' Report. *The IRM Quarterly,* **9**(4), pp2+6.

Wait, J. R., (1951). A conducting sphere in a time varying magnetic field: *Geophysics*, **16**, no. 4, p. 666-672.

Worm, H.-U., (1998). On the superparamagnetic-stable single domain transition for magnetite, and frequency dependence of susceptibility: *Geophys. J. Int.*, **133**, p. 201-206.

Worm, H.-U., Clark, D., and Dekkers, M. J., (1993). Magnetic susceptibility of pyrrhotite: grain size, field and frequency dependence: *Geophys. J. Int.*, **114**, p. 127–137.

* This is admittedly a bit outlandish. However, there are a limited number of reasonable ways to be wrong[6].

The *Institute for Rock Magnetism* is dedicated to providing state-of-the-art facilities and technical expertise free of charge to any interested researcher who applies and is accepted as a Visiting Fellow. Short proposals are accepted semi-annually in spring and fall for work to be done in a 10-day period during the following half year. Shorter, less formal visits are arranged on an individual basis through the Facilities Manager.

The *IRM* staff consists of **Subir Banerjee**, Professor/Director; **Bruce Moskowitz**, Professor/Associate Director; **Jim Marvin**, Senior Scientist; **Mike Jackson**, Senior Scientist and Facility Manager, and **Peat Sølheid**, Scientist.

Funding for the *IRM* is provided by the **National Science Foundation**, the **W. M. Keck Foundation**, and the **University of Minnesota**.

The *IRM Quarterly* is published four times a year by the staff of the *IRM*. If you or someone you know would like to be on our mailing list, if you have something you would like to contribute (*e.g.*, titles plus abstracts of papers in press), or if you have any suggestions to improve the newsletter, please notify the editor:

Mike Jackson
Institute for Rock Magnetism
University of Minnesota
291 Shepherd Laboratories
100 Union Street S. E.
Minneapolis, MN 55455-0128
phone: (612) 624-5274
fax: (612) 625-7502
e-mail: irm@umn.edu
www.geo.umn.edu/orgs/irm/irm.html

I R M

Institute for Rock Magnetism

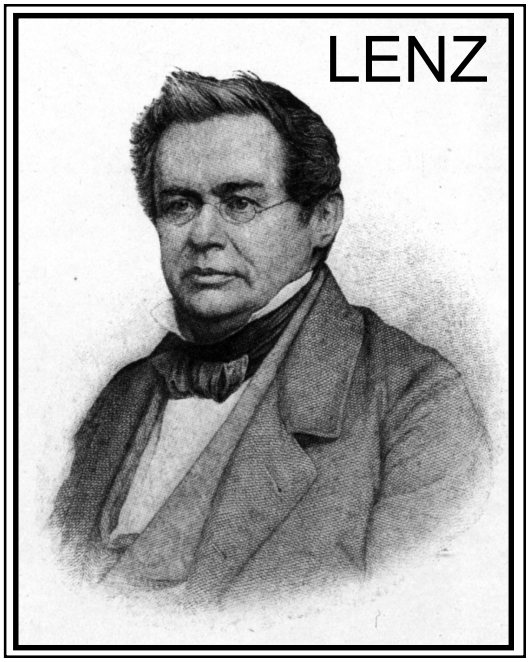

Collector's Series #25

Stine, W.M., ***The Contributions of H.F.E. Lenz to Electromagnetism,*** *Acorn Press, Philadelphia, 1923.*

Carhenge, in Alliance Nebraska, is an "exact" scale model of Stonehenge, complete with trilithons, Sarsen stones, an Aubrey circle, and a '62 Cadillac heelstone. It was conceived by artist Jim Reinders as a memorial to his father, who had lived on a farm where the monument was ultimately built in 1987. Image from http://www.roadsideamerica.com/set/OVERhenges.html

The IRM Quarterly

University of Minnesota
291 Shepherd Laboratories
100 Union Street S. E.
Minneapolis, MN 55455-0128
phone: (612) 624-5274
fax: (612) 625-7502
e-mail: irm@umn.edu
www.geo.umn.edu/orgs/irm/irm.html

Nonprofit Org.
U.S Postage
PAID
Mpls., MN
Permit No. 155